

High Efficiency Photon Number Detection for Quantum Information Processing

Edo Waks,¹ Kyo Inoue,^{1,2} William D. Oliver,¹ Eleni Diamanti,¹ and Yoshihisa Yamamoto^{1,2}

¹*Quantum Entanglement Project, ICORP, JST, E.L. Ginzton Laboratories, Stanford University, Stanford, CA 94305*

²*NTT basic research, Atsugi, Kanagawa, Japan*

(Dated: October 30, 2018)

The Visible Light Photon Counter (VLPC) features high quantum efficiency and low pulse height dispersion. These properties make it ideal for efficient photon number state detection. The ability to perform efficient photon number state detection is important in many quantum information processing applications, including recent proposals for performing quantum computation with linear optical elements. In this paper we investigate the unique capabilities of the VLPC. The efficiency of the detector and cryogenic system is measured at 543nm wavelengths to be 85%. A picosecond pulsed laser is then used to excite the detector with pulses having average photon numbers ranging from 3-5. The output of the VLPC is used to discriminate photon numbers in a pulse. The error probability for number state discrimination is an increasing function of the number of photons, due to buildup of multiplication noise. This puts an ultimate limit on the ability of the VLPC to do number state detection. For many applications, it is sufficient to discriminate between 1 and more than one detected photon. The VLPC can do this with 99% accuracy.

PACS numbers:

INTRODUCTION

Optical quantum information processing is one of the most rapidly developing segments of quantum information to date. The photon offers many distinct advantages over other implementations of a quantum bit (qubit). It is very robust to environmental noise, and can be transmitted over very long distances using optical fibers. For this reason the photonic qubit is the exclusive information carrier for quantum cryptography applications. Recent theoretical developments have also shown that single photons, combined with only linear optical components and photon counters, can be used to implement scalable quantum computers.

At the heart of any optical quantum information processing application is the ability to detect photons. Photon counters are an essential tool for virtually all quantum optics experiments. A photon counter absorbs a single photon, and outputs a macroscopic current that can be processed by subsequent digital circuits. To date, photomultiplier tubes (PMTs) and avalanche photodiodes (APDs) are the most common photon counters. In a PMT, a photon scatters a single electron from a photocathode. The electron is multiplied by successive scattering off of dynodes in order to generate a macroscopic current. PMTs are known to have superb time resolution and low pulse height dispersion, yet they typically suffer from low detection efficiencies. Optimal quantum efficiencies for a PMT typically do not exceed 40%. Avalanche photodiodes feature higher quantum efficiencies. In an APD, a photon creates a single electron hole pair in a semiconductor pn junction. An avalanche breakdown mechanism multiplies this electron-hole pair into a large current. APDs can have quantum efficiencies as high as 75%. The main limitations of APDs is that they

have a relatively long dead time (35ns), and large pulse height dispersion. If two photons are simultaneously absorbed by the APD, the output pulse will not differ from the case when only one is absorbed. Thus, APDs cannot distinguish between one and more than one photon if all of the photons land within the dead time of the detector. We refer to such detectors as threshold detectors.

Recently, a new type of photon detector, the Visible Light Photon Counter (VLPC), has been shown to have some unique capabilities that conventional PMTs and APDs don't have. The VLPC features high quantum efficiencies (94%), and low pulse height dispersion [1, 2]. This latter property makes the VLPC useful for photon number detection [3]. Unlike an APD, if two photons are simultaneously absorbed by the VLPC, the detector outputs a voltage pulse which is twice as high. This behavior continues for higher photon numbers. Thus, the voltage pulse of the VLPC carries information about photon number. We refer to this type of detector as a photon number detector, in contrast to threshold detectors discussed previously.

Photon number detection is very useful for quantum information processing. It has applications in quantum cryptography, particularly in conjunction with parametric down-conversion. It is also an important element for linear optical quantum computation (LOQC) as proposed by Knill, Laflamme, and Milburn [4]. Many of the basic building blocks for this proposal fundamentally rely on the ability to distinguish between one and more than one photon with high quantum efficiency [5].

There are several unique aspects of the VLPC which allow it to do photon number detection. First, the VLPC is a large area detector, whose active area is about 1mm in diameter. When a photon is detected, a dead spot of several microns in diameter is formed on the detector surface, leaving the rest of the detector available for

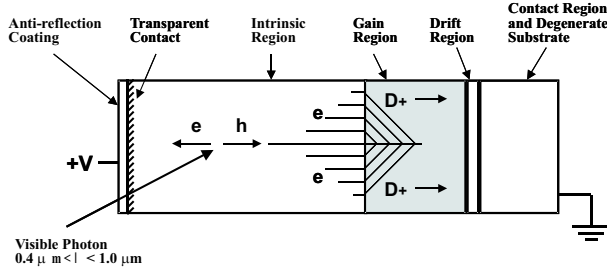


FIG. 1: Schematic of structure of the VLPC detector

subsequent detection events. If more than one photon is incident on the detector, it will be able to detect all the photons as long as the probability that multiple photons land on the same location is small. This is a good approximation if the light is not too tightly focussed on the detector surface. In this respect the VLPC is similar to a large array of beamsplitters and threshold detectors.

There is, however, one major distinction between the VLPC and a large detector array. In an array, we can address the signal from each counter individually. In contrast, we cannot individually access each spot on the VLPC surface. Instead, the current from the entire detector is summed and accessed through a single output. We must use the height or area of the output pulse to infer the photon number. This makes the noise properties of the detector critical for photon number detection. When independent noisy voltages are summed the noise builds up. This degrades the number resolution capability of the detector, and ultimately puts a limit on the number of incident photons that can be resolved. It is important to measure this limitation in order to assess the capability of the detector to perform quantum information processing tasks. For this we need to consider the noise properties of the VLPC.

The noise properties of a photon counting system are ultimately limited by the internal multiplication noise of the detector. Photon counters typically rely on an internal multiplication gain to create a large current spike from a single photoionization event. These gain mechanisms create internal multiplication noise, meaning that the current spikes generated by a photodetection event will fluctuate in height and area. In order to do accurate photon number detection, this multiplication noise must be low. Fortunately, the VLPC has been measured to have nearly noise-free multiplication [1].

VLPC OPERATION PRINCIPLE

Figure 1 shows the structure of the VLPC detector. Photons are presumed to come in from the left. The VLPC has two main layers, an intrinsic silicon layer and a lightly doped arsenic gain layer. The top of the in-

trinsic silicon layer is covered by a transparent electrical contact and an anti-reflection coating. The bottom of the detector is a heavily doped arsenic contact layer, which is used as a second electrical contact.

A single photon in the visible wavelengths can be absorbed either in the intrinsic silicon region or in the doped gain region. This absorption event creates a single electron-hole pair. Due to a small bias voltage (6-7.5V) applied across the device, the electron is accelerated towards the transparent contact while the hole is accelerated towards the gain region. The gain region is moderately doped with As impurities, which are shallow impurities lying only 54meV below the conduction band. The device is cooled to an operation temperature of 6-7K, so there is not enough thermal energy to excite donor electrons into the conduction band. These electrons are effectively frozen out in the impurity states. However, when a hole is accelerated into the gain region it easily impact ionizes these impurities, kicking the donor electrons into the conduction band. Scattered electrons can create subsequent impact ionization events resulting in avalanche multiplication.

One of the nice properties of the VLPC is that, when an electron is impact ionized from an As impurity, it leaves behind a hole in the impurity state, rather than in the valence band as in the case of APDs. The As doping density in the gain region is carefully selected such that there is partial overlap between the energy states of adjacent impurities. Thus, a hole trapped in an impurity state can travel through conduction hopping, a mechanism based on quantum mechanical tunnelling. This conduction hopping mechanism is slow, the hole never acquires sufficient kinetic energy to impact ionize subsequent As sites. The only carrier that can create additional impact ionization events is the electron kicked into the conduction band. Thus, the VLPC has a natural mechanism for creating single carrier multiplication, which is known to significantly reduce multiplication noise [6]. We will return to this point in the upcoming sections.

One of the disadvantages of using shallow As impurities for avalanche gain is that these impurities can easily be excited by room temperature thermal photons. IR photons with wavelengths of up to $30\mu\text{m}$ can directly optically excite an impurity. These excitations can create extremely high dark count levels. The bi-layer structure of the VLPC helps to suppress this. A visible photon can be absorbed both in the intrinsic and doped silicon regions. An IR photon, on the other hand, can only be absorbed in the doped region, as its energy is smaller than the bandgap of intrinsic silicon. Thus, the absorption length of IR photons is much smaller than visible photons. This suppresses the sensitivity of the device to IR photons to about 2%. Despite this suppression, the background thermal radiation is very bright, requiring orders of magnitude of additional suppression. In the

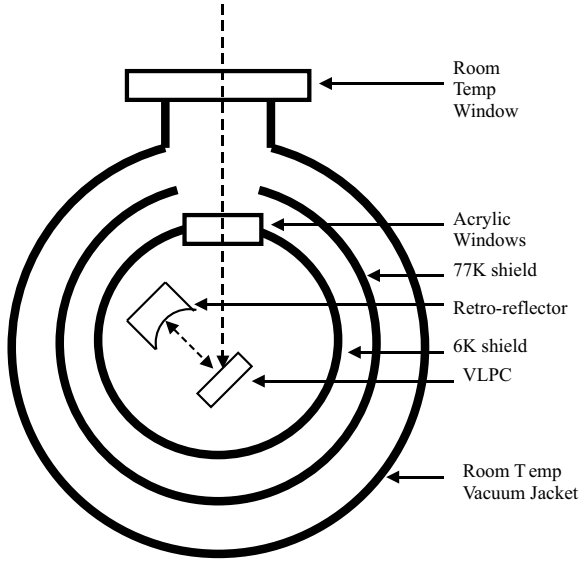


FIG. 2: Schematic of cryogenic setup for VLPC.

next section we will discuss how this is achieved.

CRYOGENIC SYSTEM FOR OPERATING THE VLPC

In order to operate the VLPC we must cool it down to cryogenic temperatures to achieve carrier freezeout of the As impurities. We must also shield it from the bright room temperature thermal radiation which it is partially sensitive to. This is achieved by the cryogenic setup shown in Figure 2.

The VLPC is held in a helium bath cryostat. As small helium flow is produced from the helium bath to the cryostat cold finger by a needle valve. The helium bath is surrounded by a nitrogen jacket for radiation shielding. This improves the helium hold time. A thermal shroud, cooled to 77K by direct connection to the nitrogen jacket, covers the VLPC and low temperature shielding. This shroud is intended to improve the temperature stability of the detector by reducing the thermal radiation load. A hole at the front of the shroud allows photons to pass through. The detector itself is encased in a 6K shield made of copper. The shield is cooled by direct connection to the cold plate of the cryostat. The front windows of the 6K radiation shield, which are also cooled down to this temperature, are made of acrylic plastic. This material is highly transparent at optical frequencies, but is almost completely opaque from $2-30\mu m$. The acrylic windows provide us with the required filtering of room temperature IR photons for operating the detector. We achieve sufficient extinction of the thermal background using 1.5-2 cm of acrylic material. In order to eliminate reflection losses from the window surfaces, the win-

dows are coated with a broadband anti-reflection coating centered at 532nm. Room temperature transmission measurements indicate a 97.5% transmission efficiency through the acrylic windows. However, the performance of the anti-reflection coating degrades when the windows are cooled down to cryogenic temperatures. Low temperature reflection measurements indicate a 7% reflection loss. This increased loss is attributed to changes in the dielectric constant of the material, resulting in a worse impedance match for the anti-reflection coating. Better engineering of the anti-reflection coating could help eliminate these losses.

The surface of the VLPC has a broadband anti-reflection coating centered around 550nm. Nevertheless, due to the large index mismatch between silicon and air, there is still substantial reflection losses on the order of 10%, even at the correct wavelength. In order to eliminate this reflection loss, the detector is rotated 45 degrees to the direction of the incoming light. A spherical refocusing mirror, with reflectance exceeding 99%, is used to redirect reflected light back onto the detector surface. A photon must reflect twice off of the surface in order to be lost, reducing the reflection losses to less than 1%.

The VLPC features high multiplication gains of about 30,000 electrons per photo-ionization event. Nevertheless, this current must be amplified significantly in order to achieve sufficiently large signal for subsequent electronics. The current is amplified by a series of broadband RF amplifiers. In order to minimize the thermal noise contribution from the amplifiers, the first amplification stage consists of a cryogenic pre-amplifier, which is cooled to 4K by direct thermalization to the helium bath of the cryostat. The amplifier features a noise figure of 0.1 at the operating frequencies of $30 - 500 MHz$, with a gain of roughly 20dB. The cryogenic amplifier is followed by additional commercial room temperature RF amplifiers. The noise properties of these subsequent amplifiers is not as important since the signal to noise ratio is dominated by the first cryogenic amplification stage. Using such a configuration, we achieve a 120mV pulse with a 3ns duration when using 62dB of amplifier gain.

QUANTUM EFFICIENCY AND DARK COUNTS OF THE VLPC

The quantum efficiency of the VLPC has already been studied at 650nm [2]. Quantum efficiencies (QE) as high as 88% have been reported. The dark counts at this peak QE were 20,000 1/s. Here we present measurements using a different operating wavelength of 543nm, and a different cryogenic setup. As a quick summary of what we will discuss, we observe raw quantum efficiencies as high as 85% at this operating wavelength, with dark count rates of roughly 20,000 1/s. When correcting for reflection losses from the windows and detector surface, we

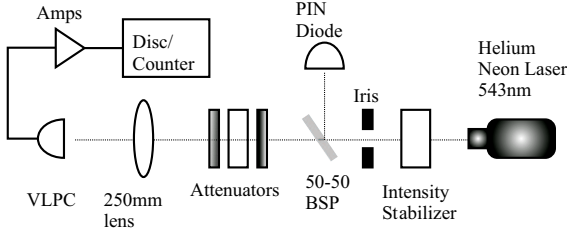


FIG. 3: Experimental setup to measure quantum efficiency of the VLPC.

estimate an intrinsic quantum efficiency of 93%. These numbers are consistent with previous measurements.

The setup for measuring the quantum efficiency of the VLPC is shown in Figure 3. We use a helium neon laser with an output wavelength of 543nm as a light source for the measurement. An intensity stabilizer is used to stabilize the output of the laser to within about 0.1%. A 50-50 beamsplitter is then used to send part of the laser to a calibrated PIN diode to measure the power. The power reading from the diode is accurate to within a 2% calibration error. Using this power reading we can calculate the photon flux N , in units of photons per second. This is given by the relation

$$N = \frac{\lambda P}{hc}, \quad (1)$$

where λ is the wavelength of the laser, P is the power measured by the PIN diode, h is Planck's constant, and c is the velocity of light in vacuum.

The laser is attenuated by a series of carefully calibrated neutral density (ND) filters down to a flux of approximately 20,000 cps. The attenuation required for this is on the order of 10^{-9} . This flux is sufficiently small to ensure that we are well within the linear regime of the VLPC. At count rates exceeding 10^5 cps, the efficiency of the VLPC will begin to drop due to dead time effects. To measure the efficiency of the VLPC we record the count rates of the detector, which we label N_c , as well as the background counts N_d , which are measured by blocking the laser. The measured efficiency η is given by

$$\eta = \frac{N_c - N_d}{\alpha N}, \quad (2)$$

where α is the transmission efficiency of the ND filters.

In Figure 4, we show the measured quantum efficiency of the VLPC as a function of applied bias voltage across the device. Efficiencies are given for several different operating temperatures. At 7.4V bias the VLPC attains its highest quantum efficiency of 85%. As the bias voltage is decreased the quantum efficiency also decreases. The reason for this is that, at lower bias voltages, electrons created by impact ionization of the initial hole are less

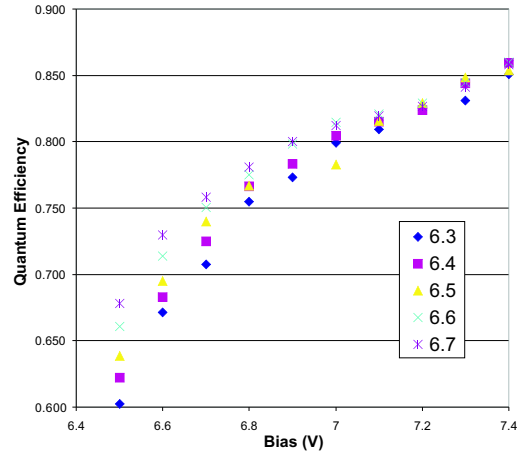


FIG. 4: Quantum efficiency of VLPC vs. bias voltage for different temperatures.

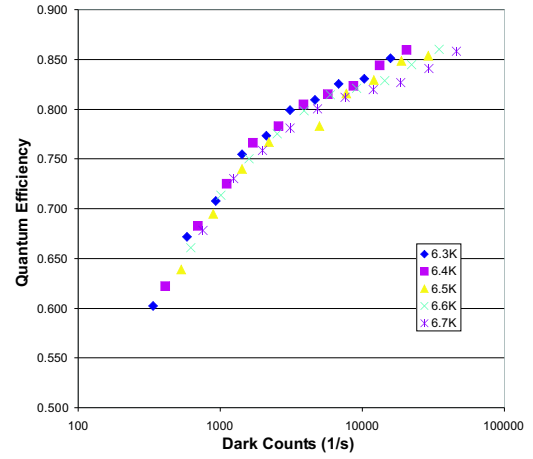


FIG. 5: Quantum efficiency of VLPC vs. dark counts for different temperatures.

likely to accumulate sufficient kinetic energy in the gain region to trigger an avalanche. The bias voltage cannot be increased beyond 7.4V. Beyond this bias the VLPC breaks down, resulting in large current flow through the device. This breakdown is attributed to direct tunnelling of electrons from impurity sites into the conduction band.

One will notice that as the temperature is decreased, more bias voltage is required to achieve the same quantum efficiency. This effect is attributed to a temperature dependence of the dielectric constant of the device, which results in a change in the electric field intensity in the gain region of the VLPC. As the temperature is decreased, it is speculated that the dielectric constant increases, requiring higher bias voltage to achieve the same electric field intensity. This conjecture is supported by the measurements shown in Figure 5. In this figure we

plot the quantum efficiency as a function of dark counts, instead of bias voltage. Data is shown for the different temperatures. Increasing the bias voltage results not only increased quantum efficiency, but also in increased dark counts. Increasing the temperature also increases both quantum efficiency and dark counts. But if we plot the quantum efficiency as a function of dark counts, as is done in Figure 5, the data for different temperatures all lie along the same curve. This suggests that the quantum efficiency and dark counts both depend on a single parameter, the electric field intensity in the gain region. The temperature and bias voltage dependence of this parameter result in the behavior shown in Figure 4. From Figure 5 we see that the maximum quantum efficiency of 85% is achieved at a dark count rate of roughly 20,000 cps.

In order to infer the actual efficiency of the VLPC alone, we must correct for all other losses in our detection system. The acrylic windows are a big source of loss. As mentioned previously, the windows add a 7% reflection loss to our measurement. In addition to this loss we have a reflection loss of 1% due to the VLPC surface, despite the retro-reflector. Other effects such as detector dead time and beam focussing should contribute only negligibly small corrections to the device efficiency. Thus, the efficiency of the VLPC detector itself is estimated to be 93% at 543nm wavelengths.

NOISE PROPERTIES OF THE VLPC

When a photon is absorbed in a semi-conductor material, it creates a single electron hole pair. The current produced by this single pair of carriers is, in almost all cases, too weak to observe due to thermal noise in subsequent electronic components. Single photon counters get around this problem by using an internal gain mechanism to multiply the initial pair into a much greater number of carriers. Avalanche photodiodes achieve this by an avalanche breakdown mechanism in the depletion region of the diode. Photomultipliers instead rely on successive scattering off of dynodes. The VLPC achieves this gain by impact ionization of shallow arsenic impurities in silicon.

All of the above gain mechanism have an intrinsic noise process associated with them. That is, a single ionization event does not produce a deterministic number of electrons. The number of electrons the device emits fluctuate from pulse to pulse. This internal noise is referred to as excess noise, or gain noise. The amount of excess noise that a device features strongly depends on the mechanism in which gain is achieved. The excess noise is typically quantified by a parameter F , referred to as the excess noise factor (ENF). The ENF is mathematically defined

as

$$F = \frac{\langle M^2 \rangle}{\langle M \rangle^2}, \quad (3)$$

where M is the number of electrons produced by a photo-ionization event, and the brackets notation represents a statistical ensemble averages. Noise free multiplication is represented by $F = 1$. In this limit, a single photo-ionization event creates a deterministic number of additional carriers. Fluctuations in the gain process will result in an ENF exceeding 1.

The noise properties of an avalanche photo-diode are well characterized. The first theoretical study of such devices was presented by McIntyre in 1966 [6]. McIntyre studied avalanche gain in the "Markov" limit. In this limit, the impact ionization probability for a carrier in the depletion region is a function of the local electric field intensity at the location of the carrier. In this sense, each impact ionization event is independent of past history. Under this assumption the ENF of an APD was calculated. The ENF depends on the number of carriers that can participate in the avalanche process. If both electrons and holes are equally likely to impact ionize, then $F \approx \langle M \rangle$. In the large gain limit the ENF is very big. Restricting the impact ionization process to only electrons or holes significantly reduces the gain noise. In this ideal limit, we have $F = 2$. This limit represents the best noise performance achievable within the Markov approximation.

PMTs are known to have better noise characteristics than APDs. The ENF of a typical PMT is around 1.2. This suppressed noise is because, in a PMT, a carrier is scattered off of a fixed number of dynodes. The only noise in the process is the number of electrons emitted by each dynode per electron.

The multiplication noise properties of the VLPC have been previously studied. Theoretical studies of the multiplication noise have predicted that the VLPC should feature suppressed avalanche multiplication noise. This is due to two dominant effects. First, because only electrons can cause impact ionization, the VLPC features a natural single carrier multiplication process. Second, the VLPC does not require high electric field intensities to operate. This is because impact ionization events occur off of shallow arsenic impurities which are only 54meV from the conduction band. Thus, carriers do not have to acquire a lot of kinetic energy in order to scatter the impurity electrons. Because of the lower electric field intensities, a carrier requires a fixed amount of time before it can generate a second impact ionization. This delay time represents a deviation from the Markov approximation, and is predicted to suppress the multiplication noise [7]. The ENF of the VLPC has been experimentally measured to be less than 1.03 in [1]. Thus, the VLPC features nearly noise free multiplication, as predicted by theory. This low noise property will play an important

role in multi-photon detection, which we discuss next.

MULTI-PHOTON DETECTION WITH THE VLPC

The nearly noise-free avalanche gain process of the VLPC opens up the door to perform multi-photon detection. When more than one photon is detected by the VLPC, we expect the number of electrons emitted by the detector to be twice that of a single photon detection. If the photons arrive within a time interval which is much shorter than the electronic output pulse duration of the detection system, then we expect to see a detection pulse which is twice as high.

In the limit of noise free multiplication, this would certainly be the case. A single detection event would create M electrons, while a two photon event would create $2M$ electrons. Higher order photon number detections would follow the same pattern. After amplification, the area or height of the detector pulse would allow us to perfectly discriminate the number of detected photons, even if they arrive on extremely short time scales.

In the presence of multiplication noise, the situation becomes more complicated. The pulse height of a one photon pulse will fluctuate, as will that of a two photon pulse. There becomes a finite probability that we only detect one photon, but due to multiplication noise the height of the pulse appears to be more consistent with a two photon event, and vice versa. Our ability to discriminate the number of detected photons becomes a question of signal to noise ratio.

There are ultimately two effects which will limit multi-photon detection. One is the quantum efficiency of the detector. If we label the quantum efficiency as η , then the probability of detecting n photons is given by η^n , assuming detector saturation is negligible. Thus, the detection probability is exponentially small in η . For larger n this may produce extremely low efficiencies. The second limitation is the electrical detection noise, as previously discussed. There are two contributions to the electrical noise. One is the excess noise of the detector, and the other is electrical noise originating from amplifiers and subsequent electronics. The latter can in principle be eliminated by engineering ultra-low noise circuitry. The former, however, is a fundamental property of the detector which cannot be circumvented, short of engineering a different detector with better noise properties.

In the absence of detection inefficiency and amplifier noise, the multiplication noise will ultimately put a limit on how many simultaneous photons we can detect. Defining σ_m as the standard deviation of the multiplication gain, the fluctuations of an n photon peak will be given by $\sqrt{n}\sigma_m$. This is because the n photon pulse is simply the sum of n independent single photon pulses from different locations of the VLPC active area. Summing the

pulses also causes the variance to sum, resulting in the buildup of multiplication noise. The mean pulse height separation between the n photon peak and the $n-1$ photon peak, however, is constant. It is simply proportional to $\langle M \rangle$, the average multiplication gain. At some sufficiently high photon number, the fluctuations in emitted electrons will be so large that there is little distinction between an n and $n-1$ photon event. We can arbitrarily establish a cutoff number at the point where the fluctuations in emitted electrons is equal to the average difference between an n and $n-1$ photon detection event. In this limit, the maximum photon number we can detect is

$$N_{max} = \frac{1}{F-1}. \quad (4)$$

Using the above condition as a cutoff, we see that even an ideal APD with $F = 2$ cannot discriminate between 1 and 2 photon events. A PMT with $F = 1.2$ could potentially be useful for up to 5 photon detection, but due to low quantum efficiencies of PMTS, this is typically impractical. The VLPC, with $F < 1.03$ could potentially discriminate more than 30 photons. Furthermore it could potentially do this with 93% quantum efficiency. However, this limit is difficult to approach due to electronic noise contribution from subsequent amplifiers.

CHARACTERIZING MULTI-PHOTON DETECTION CAPABILITY

The multi-photon detection capability of the VLPC has been previously studied. Early studies used long light pulse excitations, with poor electronic time resolution so that multiple photons appeared as a single electronic pulse [8]. Later studies used twin photons generated from parametric down-conversion, which arrive nearly simultaneous, to investigate multi-photon detection [3]. These studies restricted their attention to one and two photon detection. Higher photon numbers were not considered.

The experiment described below measures the photon number detection capability of the VLPC when excited by multiple photons. Figure 6 shows the experimental setup. A Ti:Sapphire laser, emitting pulses of about 3ps duration, is used. The duration of the optical pulses are much shorter than the electrical pulse of the VLPC detector, which is 2ns. A pulse picker is used to down-sample the repetition rate of the laser from 76MHz to 15KHz. This is done in order to avoid saturation of the detector. A synchronous countdown module, which is used as the pulse picking signal, is also used to trigger a boxcar integrator. The output of the VLPC is amplified by the amplifier configuration discussed earlier. The amplified signal is integrated by a boxcar integrator. The integrated value of a pulse is proportional to the number of electrons emitted by the detector, as long as amplifier

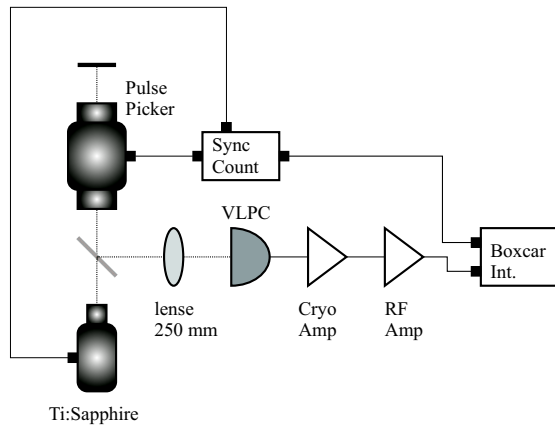


FIG. 6: Experimental setup to measure multi-photon detection capability of the VLPC.

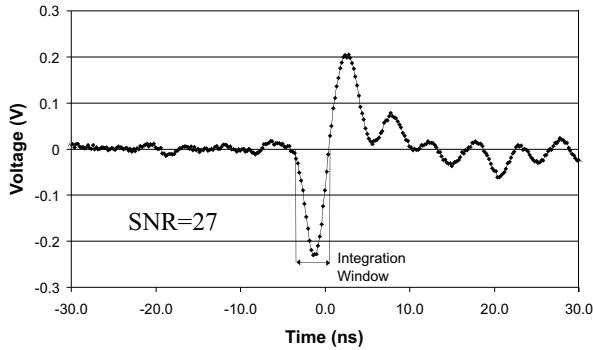


FIG. 7: Oscilloscope pulse trace of VLPC output after room temperature RF amplifiers.

saturation is negligible. The output of the boxcar integrator is digitized by an analog to digital converter, and stored on a computer.

Figure 7 shows a sample oscilloscope pulse trace of a VLPC pulse after the room temperature amplifiers. The output features an initial sharp negative peak of about 2ns full width at the half maximum. A positive overshoot follows. This positive overshoot is the result of the 30MHz high pass of the cryogenic amplifiers. If we compare the variance of the electrical fluctuations before the pulse to the minimum pulse value, we determine the signal to noise ratio (SNR) to be 27. The figure also illustrates the integration window used by the boxcar integrator, which captures only the negative lobe of the pulse.

In order to measure the multi-photon detection capability, we attenuate the laser to about 1-5 detected photons per pulse. For each laser pulse, the output of the VLPC is integrated and digitized. Figure 8 shows pulse area histograms for four different excitation powers. The area is expressed in arbitrary units determined by the

analog to digital converter. Because the pulse area is proportional to the number of electrons in the pulse, the pulse area histogram is proportional to the probability distribution of the number of electrons emitted by the VLPC. This probability distribution features a series of peaks. The first peak is a zero photon event, followed by one photon, two photons, and so on. In the absence of electronic noise and multiplication noise, these peaks would be perfectly sharp, and we would be able to unambiguously distinguish photon number. Due to electronic noise however, the peaks become broadened and start to partially overlap. The broadening of the zero photon peak is due exclusively to electronic noise. Note that the boxcar integrator adds an arbitrary constant to the pulse area, so that the zero photon peak is centered around 450 instead of 0. The one photon peak is broadened by both electronic noise and multiplication noise. Thus, the variance of the one photon peak is bigger than the zero photon peak. As the photon number increases, the width of the pulses also increases due to buildup of multiplication noise. This eventually causes the smearing out of the probability distribution at around the seven photon peak.

In order to numerically analyze the results, we fit each peak to a gaussian distribution. Theoretical studies predict that the distribution of the one photon peak is a bisigmoidal distribution, rather than a gaussian [7]. However, when the multiplication gain as large, as in the case of the VLPC, this distribution is well approximated by a gaussian. We use this approximation because higher photon number events are sums of multiple single photon events. A gaussian distribution has the nice property that a sum of gaussian distributions is also a gaussian distribution. In the limit of large photon numbers we expect this approximation to get even better due to the central limit theorem.

The most general fit would allow the area, mean, and variance of each peak to be independently adjustable. This allows too many degrees of freedom, which often results in the optimization algorithm falling into a local minimum. To help avoid this, we do not allow the average of each peak to be independently adjustable. Instead, we require the averages to be equally spaced, as would be expected from our model of the VLPC. Thus, the average of the i 'th peak, denoted x_i , is determined by the relation

$$x_i = x_0 + i\Delta - i^2\alpha. \quad (5)$$

In the above equation, x_0 is the average of the zero photon peak, Δ is the spacing between peaks, and α is a small correction factor which can account for effects such as amplifier saturation. These three parameters are all independently adjustable. In all of our fits, α was much smaller than Δ indicating the peaks are, for the most part, equally spaced.

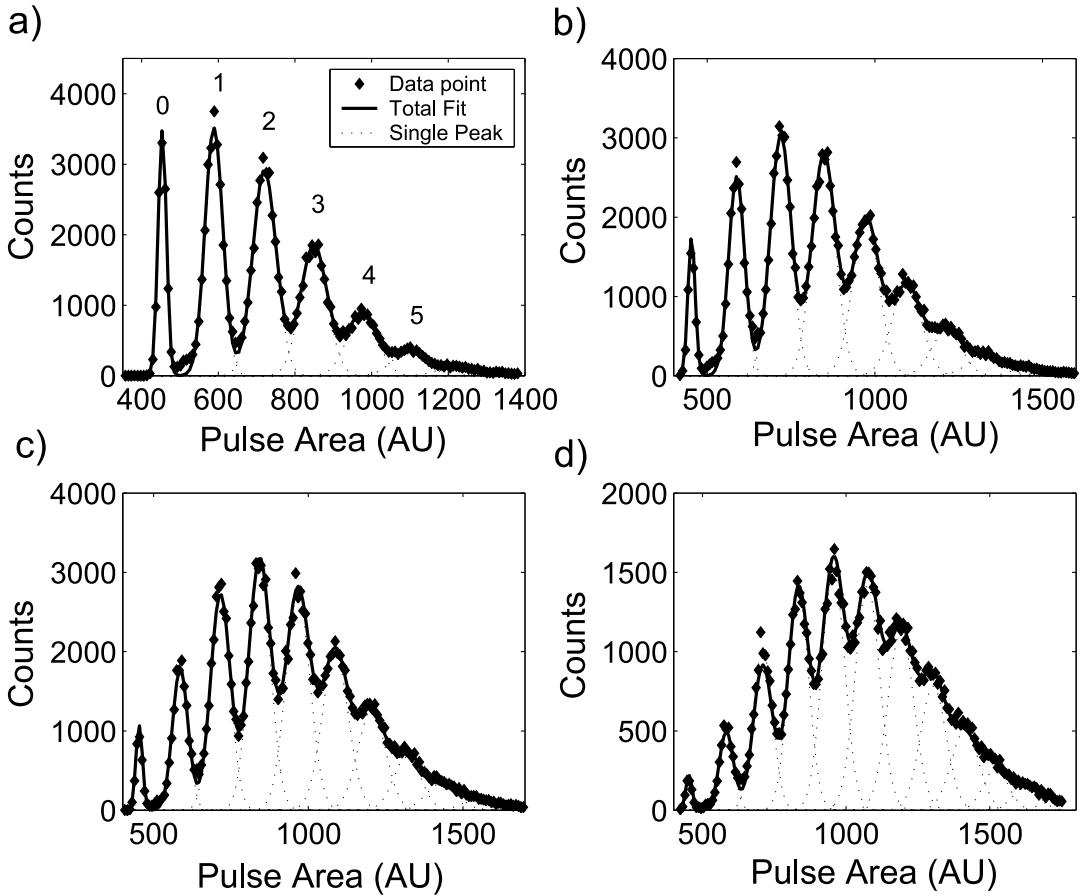


FIG. 8: Pulse area spectrum generated by the boxcar integrator for four different excitation powers. The dotted lines represent the fitted distribution of each photon number peak. The solid line is the total sum of all the peaks. Diamonds denote measured data points. Each peak represents a photon number event, starting with zero photons for the first peak.

Figure 8 shows the results of the fits for each excitation intensity. The dotted lines plot the individual gaussian distributions for the different photon numbers, and the solid line plots the sum of all of the gaussians. The diamond markers represent the measured data points. Table I shows the center value and standard deviation of the different peaks in panel c of the figure. In order to do photon number counting we must establish a decision region for each photon number state. This will depend, in general, on the a-priori photon number distribution. We consider the case of equal a-priori probability, which is the worst case scenario. For this case, the optimal decision threshold between two consecutive gaussian peaks is given by the point where they intersect. The value of

this point can be easily solved, and is given by,

$$x_d = x_i - \frac{\sigma_i^2(x_{i+1} - x_i)}{\sigma_{i+1}^2 - \sigma_i^2} + \frac{\sigma_i \sigma_{i+1} \sqrt{(x_{i+1} - x_i)^2 - 2(\sigma_{i+1}^2 - \sigma_i^2) \ln \frac{\sigma_i}{\sigma_{i+1}}}}{\sigma_{i+1}^2 - \sigma_i^2}. \quad (6)$$

The probability of error for this decision is given by the area of all other photon number peaks in the decision region. This probability is also shown in Table I.

From the data we would like to infer whether the VLPC is being saturated at higher photon numbers. If too many photons are simultaneously incident on the detector, the detector surface may become depleted of active area. This would result in a reduced quantum efficiency for higher photon numbers. In order to investigate this possibility, we add an additional constraint to the fit that the pulse areas must scale according to a Poisson distribution. Since the laser is a Poisson light source, we expect this to be the case. However, if saturation be-

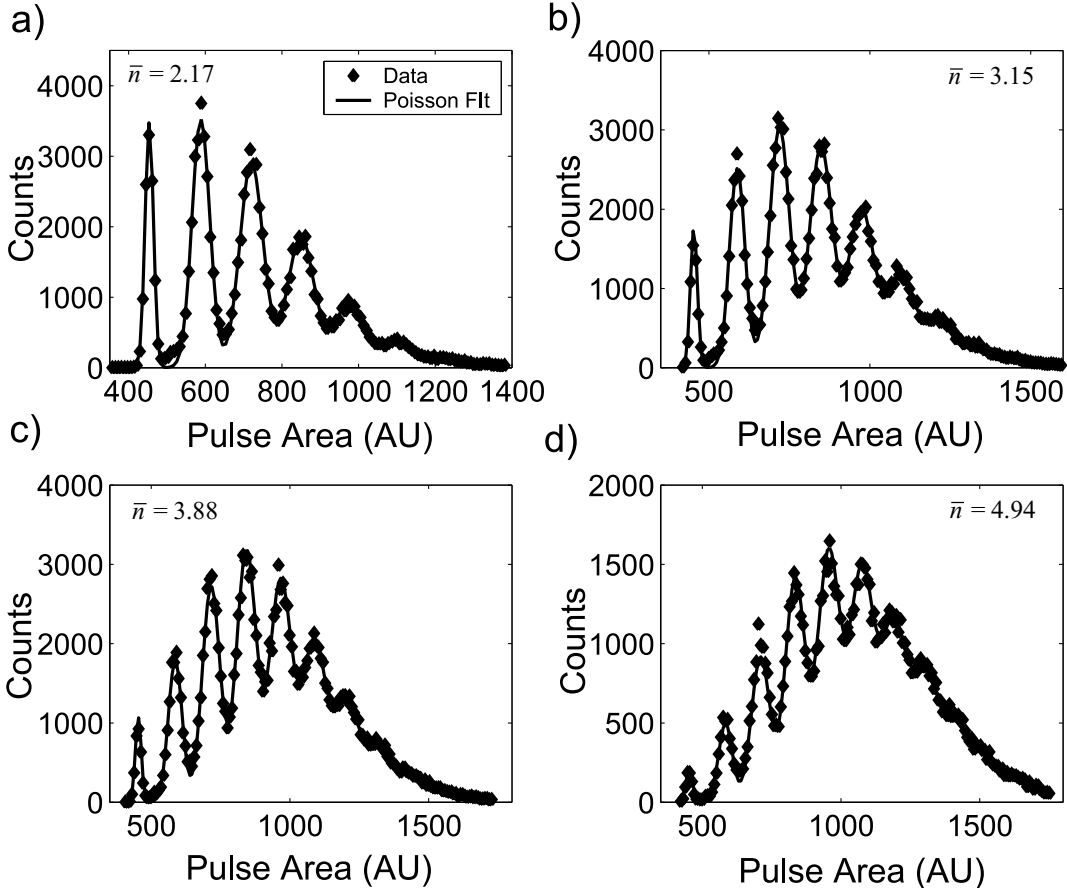


FIG. 9: Pulse area spectrum fit to Poisson constraint on normalized peak areas.

TABLE I: Results of fit for panel (c) of Figure 8.

Photon number	Avg. Area	Std. Dev.	%Error
0	0	10.6	0.01
1	135	24.8	1.1
2	275	31.7	3.4
3	416	35.3	6.1
4	561	39.0	8.5
5	709	42.2	10.6
6	859	44.5	11.3

comes a factor, we would observe a number dependant loss. This would result in deviation from Poisson detection statistics. In Figure 9 we plot the result of the fit when the peak areas scale as a Poisson distribution. One can see that the imposition of Poisson statistics does not change the fitting result in an appreciable way. Thus, we infer that detector saturation is not a strong effect at the excitation levels that we are using.

The effect of multiplication noise buildup on the pulse

height spectrum can be investigated from the previous data. In general, we expect the pulse area variance to be a linearly increasing function of photon number. This is consistent with the independent detection model, in which an n photon peak is a sum of n single photon peaks coming from different areas of the detector. To investigate the validity of this model, we plot variance as a function of photon number in Figure 10. The electrical noise variance, given by the zero photon peak, is subtracted. The variance is fit to a linear model given by

$$\sigma_i^2 = \sigma_0^2 + i\sigma_M^2. \quad (7)$$

In the above model, i is the photon number, σ_M^2 is the variance contribution from multiplication noise, and σ_0^2 is a potential additive noise term. From the data, we obtain the values $\sigma_M^2 = 276$, and $\sigma_0^2 = 246$.

A surprising aspect of this result is the large value of σ_0^2 . We expect that since electrical noise has been subtracted, the only remaining contribution to the variance is multiplication noise. If this were true, the value of σ_0 would be very small. Instead we obtain a value nearly

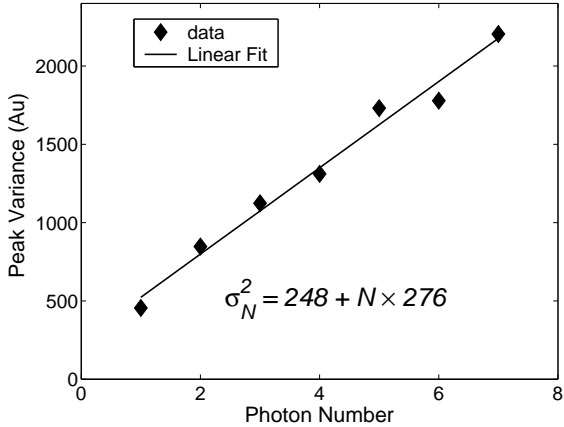


FIG. 10: Variance as a function of photon number detection. The linear relation is consistent with the independent detection model.

equal to that of σ_m^2 . This may indicate that the electrical noise is higher when the VLPC is firing, as opposed to when it's not. A change in the resistance of the device during the avalanche process may effect the noise properties of subsequent amplification circuits. Further investigation is required in order to determine whether this additive noise is fundamental to the device, or can be eliminated in principle.

The above measurements of variance versus photon number gives us a very accurate measurement of the excess noise factor F of the VLPC. Previous measurements of F for the VLPC have determined that it is less than 1.03 [1], which is nearly noise free multiplication. This number was obtained by measuring the variance of the 1 photon peak, and comparing to the mean. However, it is difficult to separate the electrical noise contribution from the internal multiplication noise using this technique. Thus, the measurement ultimately determines only an upper bound of F . By considering how the variance scales with photon numbers, as we have done in Figure 10, the multiplication noise can be accurately differentiated from additive electrical noise. This allows us to calculate an exact value for the excess noise factor. From our measurement of σ_M^2 and $\langle M \rangle$, we obtain an

excess noise factor of $F = 1.015$.

CONCLUSION

In this paper we have discussed the interesting features of the VLPC for quantum information processing. The VLPC has the potential to detect photons with quantum efficiencies approaching 93%. It also has the capability to do photon number detection, a critical feature for linear optical quantum computation. The photon number detection capability of the VLPC is fundamentally limited by internal noise processes in the device. For many applications, one does not require full photon number detection capability. It is sufficient to be able to distinguish between one and more than one detection event. The VLPC can do this with 99% accuracy. Although the requirements for fully scalable linear optical quantum computation are extremely demanding, the VLPC may find use in areas where limited quantum computational tasks are required. Such fields as quantum cryptography and quantum networking, where fully scalable computation is not always required, may be able to incorporate the VLPC to perform novel tasks.

- [1] J. Kim, Y. Yamamoto, and H. Hogue, *App. Phys. Lett.* **70**, 2852 (1997).
- [2] S. Takeuchi, J. Kim, Y. Yamamoto, and H. Hogue, *App. Phys. Lett.* **74**, 1063 (1999).
- [3] J. Kim, S. Takeuchi, Y. Yamamoto, and H. Hogue, *App. Phys. Lett.* **74**, 902 (1999).
- [4] E. Knill, R. Laflamme, and G. Milburn, *Nature* **409**, 46 (2001).
- [5] S. Bartlett, E. Diamanti, B. Sanders, and Y. Yamamoto (2002), quant-ph/0204073.
- [6] R. J. McIntyre, *IEEE Transactions of Electron Devices* **ED-13**, 164 (1966).
- [7] R. LaViolette and M. Stapelbroek, *Journal of Applied Physics* **65**, 830 (1989).
- [8] M. Atac, J. Park, D. Cline, D. Chrisman, M. Petroff, and E. Anderson, *Nuclear Instruments and Methods in Physics Research A* **314**, 56 (1992).